Molecular Therapy
Nucleic Acids
Original Article

Long Non-coding RNA LINC00628 Interacts Epigenetically with the LAMA3 Promoter and Contributes to Lung Adenocarcinoma

Shu-Feng Xu,[1,6] Yue Zheng,[2,6] Ling Zhang,[3] Ping Wang,[4] Chun-Mi Niu,[1] Tong Wu,[5] Qi Tian,[1] Xiao-Bo Yin,[1] Shan-Shan Shi,[5] Lei Zheng,[2] and Li-Ming Gao[2]

[1]Department of Respiratory, The First Hospital of Qinhuangdao, Qinhuangdao 066000, P.R. China; [2]Department of Oncology, The First Hospital of Qinhuangdao, Qinhuangdao 066000, P.R. China; [3]Department of Respiratory, Hebei Chest Hospital, Shijiazhuang 050021, P.R. China; [4]Department of Respiratory, Chinese PLA General Hospital, Beijing 100853, P.R. China; [5]Medical Students, Hebei Medical University, Shijiazhuang 050017, P.R. China

Long non-coding RNAs (lncRNAs) have emerged as key regulators of cellular progress in lung adenocarcinoma. In this study, to identify cancer-related lncRNAs and genes, we screened for those lncRNAs that were differentially expressed in lung adenocarcinoma, which revealed LINC00628 overexpression and low expression of laminin subunit alpha 3 (LAMA3). This was further validated in the cancerous tissues from patients diagnosed with lung adenocarcinoma. Thereafter, we explored the functional relevance of LINC00628 and LAMA3 in lung adenocarcinoma by analyzing the recruitment of DNA methyltransferase (DNMT) and the cellular processes of lung adenocarcinoma cells following treatments that induced LINC00628 overexpression or LINC00628 silencing or with 5-azacytidine (5-Aza, a DNMT inhibitor). The results showed that LINC00628 silencing decreased cell proliferation, migration, and invasion as well as the drug resistance of lung adenocarcinoma cells to vincristine (VCR). The results were opposite in the cells with LAMA3 demethylation induced by 5-Aza treatment. Further research indicated that LINC00628 recruited DNMT1, DNMT3A, and DNMT3B to promote the methylation of LAMA3 promoter, thereby decreasing its expression. Moreover, an *in vivo* experiment was performed in nude mice to assess the tumor growth ability and drug resistance of human lung adenocarcinoma cells. It was observed that LINC00628 silencing or 5-Aza treatment inhibited the *in vivo* tumor growth ability of the human lung adenocarcinoma cells and reduced their resistance to VCR. Altogether, our results provide evidence of a mechanism by which LINC00628 silencing exerts an inhibitory role in lung adenocarcinoma by modulating the DNA methylation of LAMA3, indicative of a novel molecular target for treatment of lung adenocarcinoma patients showing resistance to VCR.

INTRODUCTION

As the most common subtype of non-small cell lung cancer, lung adenocarcinoma accounts for over 500,000 global deaths annually.[1] The classification of intrinsic molecular subtypes of lung adenocarcinoma is based on gene expression patterns, each involving different functional pathways, and presenting variable patient outcomes.[2] In terms of etiologic factors, smoking has been regarded as the primary risk factor for lung adenocarcinoma.[3] However, in about 10% of the cases, the disease presents in those who have never smoked, suggesting genetic susceptibility and environmental exposures are both vital risk factors for cancer.[4] Notably, the gene for RNA binding motif protein 10 (RBM10), a regulator of RNA splicing, is frequently mutated in lung adenocarcinoma and acts as an oncogene. RBM10 may contribute to the pathogenesis of lung adenocarcinoma by deregulating splicing.[5] Recently, notable genetic variations have been detected among lung adenocarcinoma patients, but, as their related molecular mechanisms are not yet well understood, these have not translated to therapeutic targets for lung adenocarcinoma.[2]

Long non-coding RNAs (lncRNAs) play key roles in tumor development and progression. In particular, lncRNA HNF1A-AS1 has been implicated in the tumorigenesis of non-small cell lung carcinoma (NSCLC).[6] In addition, lncRNA metastasis-associated lung adenocarcinoma transcript 1 (MALAT1) has been used as a predictive marker for cell migration of lung cancer cells.[7] Among the newly discovered non-coding RNAs, lncRNAs have emerged as key regulators of the function of diverse cellular processes, including cell differentiation, cell growth, and disease pathogenesis.[7] lncRNAs may be involved in promoter methylation and drug resistance. For example, the expression of lncRNA LINC00472 in breast cancer is potentially mediated by promoter methylation.[8] In lung adenocarcinoma lines, promoter methylation of death associated protein kinase (DAPK) can lead to

Received 28 January 2019; accepted 1 August 2019;
https://doi.org/10.1016/j.omtn.2019.08.005.

[6]These authors contributed equally to this work.

Correspondence: Li-Ming Gao, Department of Oncology, The First Hospital of Qinhuangdao, No. 258, Wenhua Road, Haigang District, Qinhuangdao 066000, Hebei Province, P.R. China.
E-mail: Tshgaoliming@sina.com

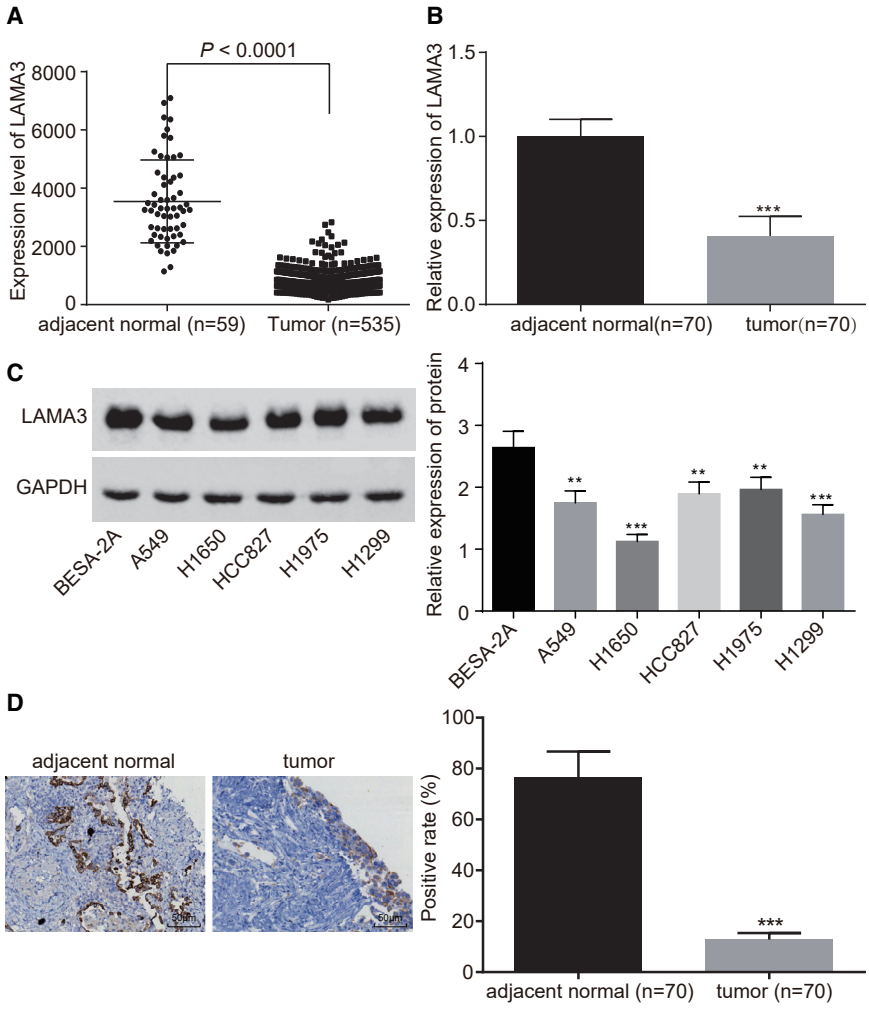

Figure 1. Low Expression of LAMA3 Is Found in Lung Adenocarcinoma Tissues and Cells

(A) TCGA database analysis of the expression of LAMA3 in lung adenocarcinoma tissues and adjacent normal tissues. (B) qRT-PCR detection of LAMA3 expression in adjacent normal tissues and lung adenocarcinoma tissues (n = 70). (C) Western blot analysis of LAMA3 protein expression in lung adenocarcinoma cell lines. (D) Positive expression rate of LAMA3 protein in lung adenocarcinoma tissues and adjacent normal tissues detected by IHC. The statistical values were measurement data, which were expressed as mean ± SD and compared with t test, n = 70; *p < 0.05; **p < 0.01; and ***p < 0.001 versus the adjacent normal tissues.

reduced expression of DAPK, thereby inducing gefitinib resistance.[9] lncRNAs and promoter activity are also implicated in epithelial function. Laminin subunit alpha 3 (LAMA3) expression is mediated by an epithelial enhancer via a synergistic effect of AP-1 binding sites.[10] LAMA3 has been implicated in the invasion and progression of tumor cells and encodes for the α3 chain of laminin-5 (α3, β3, γ2, 332), and its dysfunction manifests as a blistering skin disease similar to junctional epidermolysis bullosa in humans.[11,12] Vincristine (VCR), an anticancer agent, produces microtubule perturbation and suppresses mitosis to exert inhibitory effects on tumor growth by inducing tumor cell apoptosis. However, drug resistance in lung cancer cells can attenuate the therapeutic effects of VCR.[13] It remains unknown whether a high expression of LINC00628 can induce VCR-resistance in lung adenocarcinoma cells. Therefore, we studied the effects of LINC00628 expression on the proliferation, invasion, migration, and drug-resistance of lung adenocarcinoma cells and its relationship with the methylation of LAMA3 promoter and the VCR-resistance of lung cancer cells. This study may provide beneficial insights toward the development of novel treatments for lung adenocarcinoma patient resistant to VCR.

RESULTS

LAMA3 Is Expressed at a Low Level in Lung Adenocarcinoma Tissues and Cells

We used The Cancer Genome Atlas (TCGA) database and qRT-PCR as well as immunohistochemistry (IHC) to conduct a preliminary investigation on the expression of LAMA3 in lung adenocarcinoma tissues. The results from the TCGA database showed that LAMA3 expression in lung adenocarcinoma tissues was lower than that in adjacent normal tissues (Figure 1A). Furthermore, qRT-PCR and IHC results showed that expression of LAMA3 was decreased in lung adenocarcinoma tissues compared to the adjacent normal tissues (Figures 1B and 1D). Western blot analysis was used to examine the protein expression of LAMA3 in lung adenocarcinoma cell lines, and the results showed that, compared with the normal cell BEAS-2B, the lung adenocarcinoma cell lines A549, H1650, HCC827, H1975, and H1299 showed decreased protein expression of LAMA3 (Figure 1C) ($p < 0.05$). These results indicated the critical role of LAMA3 in the occurrence and development of lung adenocarcinoma.

Low Expression of LAMA3 Is Accompanied by High Expression of LINC00628 in Lung Adenocarcinoma

Using the Multi Experiment Matrix (MEM) website and the Kyoto Encyclopedia of Genes and Genomes (KEGG) database, we also determined the expression of LINC00628, a co-factor of LAMA3 in the phosphoinositide 3-kinase (PI3K)-Akt signaling pathway, in lung adenocarcinoma tissues (Figure 2A). The results from the TCGA database showed that LINC00628 was highly expressed in lung adenocarcinoma patients as compared to normal control subjects (Figure 2B). Furthermore, qRT-PCR verified that LINC00628 was overexpressed in human lung adenocarcinoma

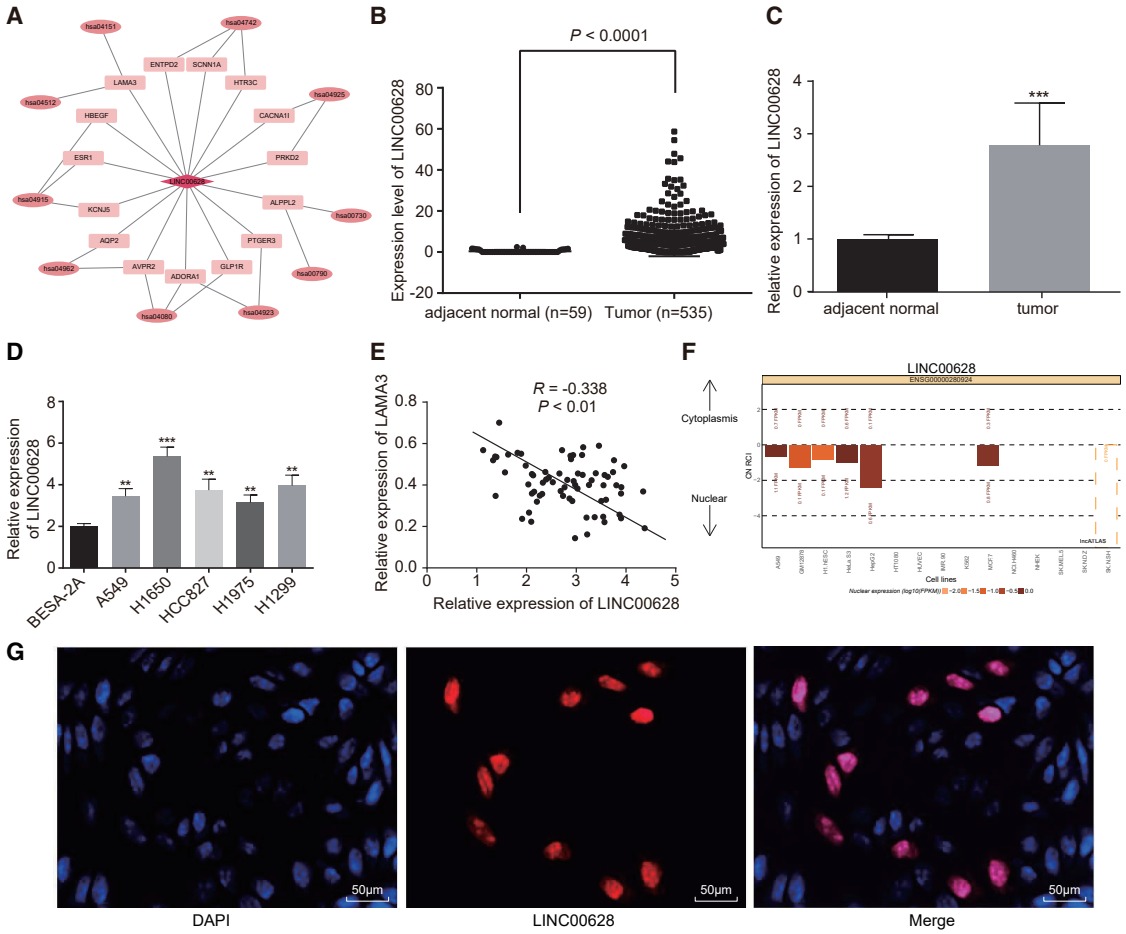

Figure 2. Low Expression of LAMA3 Is Associated with High Expression of LINC00628 in Lung Adenocarcinoma

(A) Bioinformatics analysis of LAMA3 and LINC00628, hsa04151:PI3K-Akt signaling pathway. (B) TCGA database analysis of LINC00628 expression in lung adenocarcinoma tissues and adjacent normal tissues. (C) Expression of LINC00628 in lung adenocarcinoma tissues and adjacent normal tissues, which was normalized to GAPDH expression. (D) LINC00628 expression in normal cell BEAS-2B and lung adenocarcinoma cell lines A549, H1650, HCC827, H1975, and H1299. (E) Correlation of LINC00628 and LAMA3 in human lung adenocarcinoma tissues analyzed with the Pearson correlation coefficient. (F) The location of LINC00628 in cells analyzed by sub-cell location website. (G) The location of LINC00628 in cells analyzed by FISH (400×) and DAPI-represented nucleic localization. The statistical values were measurement data, which were expressed as mean ± SD and compared with t test, n = 70; *p < 0.05; **p < 0.01; and ***p < 0.001 versus the adjacent normal tissues.

tissues (Figure 2C) and also in the lung adenocarcinoma cell lines (A549, H1650, HCC827, H1975, and H1299) (Figure 2D) ($p < 0.05$). In addition, a negative correlation was observed between the expression levels of LINC00628 and LAMA3 in lung adenocarcinoma tissues (Figure 2E). The lncRNA sub-cell location website exhibited that LINC00628 was predominantly located in the nucleus (Figure 2F), which was further verified in our results of fluorescence *in situ* hybridization (FISH) assay using the H1650 cells (Figure 2G). These results showed that LINC00628 was upregulated in lung adenocarcinoma and was correlated with reduced LAMA3 expression. Subsequently, we analyzed the correlation of expression of LINC00628 and LAMA3 to the clinicopathological features of patients diagnosed with lung adenocarcinoma and found that the LINC00628 and LAMA3 expression levels were correlated with the tumor size, clinical stage, as well as lymph node metastasis, but not correlated with the age and gender of the patients (Table 1).

Overexpressed LINC00628 Inhibits LAMA3

After transfection of the lung adenocarcinoma cell line H1650 with vectors carrying LINC00628, qRT-PCR was performed to measure the expression levels of LINC00628. The results showed that the LINC00628 expression in the transfected cells was significantly higher than the expression in the cells that served as negative control (NC) (Figure 3A). H1650 cells were transfected with sh-LINC00628 sequence (a shRNA vector against LINC00628), and the results of qRT-PCR and western blot analysis showed that LINC00628 expression in the transfected cells was lower than the expression in the cells that served as NC (Figure 3B). Also, the expression of LAMA3

Table 1. Relation between LINC00628 and LAMA3 Expression and Clinicopathological Features of Lung Adenocarcinoma Patients

Clinicopathological Features	Patients (n = 70)	LINC00628	p Value	LAMA3	p Value
Age (y)					
≤60	31	2.53 ± 0.31	>0.05	0.36 ± 0.10	>0.05
> 60	39	2.46 ± 0.38	>0.05	0.32 ± 0.10	>0.05
Gender					
Male	29	2.53 ± 0.31	>0.05	0.36 ± 0.10	>0.05
Female	41	2.46 ± 0.38	>0.05	0.32 ± 0.10	>0.05
Tumor Size (cm)					
≥3	23	2.53 ± 0.31	>0.05	0.36 ± 0.10	>0.05
< 3	47	1.46 ± 0.38	>0.05	0.49 ± 0.10	>0.05
TNM Stage					
I-II	50	1.53 ± 0.31	>0.05	0.46 ± 0.10	>0.05
III-IV	20	2.46 ± 0.38	>0.05	0.30 ± 0.10	>0.05
Lymph Node Metastasis					
Yes	19	2.53 ± 0.31	>0.05	0.36 ± 0.10	>0.05
No	51	1.46 ± 0.38	>0.05	0.49 ± 0.10	>0.05

LAMA3, laminin subunit alpha 3; TNM, tumor node metastasis.

significantly declined after transfection of LINC00628 (Figures 3C, 3I, and 3J).

Similarly, the lung adenocarcinoma cell line H1650 was transfected with vectors carrying LAMA3, and qRT-PCR and western blot analyses were performed to measure the expression levels of LINC00628 and LAMA3 in these cells. Upon LAMA3 transfection, the expression of LAMA3 was significantly higher than the expression in cells that served as NC (Figure 3D). The experiment was conducted for the H1299 cell line in a similar manner, and the results were consistent with the results of the H1650 cell line (Figures 3E–3J).

These results indicate that H1650 cells and H1299 cells could be successfully transfected with LINC00628 and LAMA3 and overexpressed LINC00628 could inhibit the expression of LAMA3.

Reduction of LINC00628 and Overexpression of LAMA3 Inhibit the Proliferation, Migration, and Invasion along with EMT of Lung Adenocarcinoma Cells

Western blot analysis was performed for the H1650 and H1299 cell lines, and the results revealed that, compared with cells that served as controls, transfection with LINC00628 led to a decreased expression of LAMA3 ($p < 0.05$), while transfection with sh-LINC00628 showed increased expression of LAMA3 ($p < 0.05$). The cells with restored LAMA3 showed significantly higher LAMA3 expression ($p < 0.05$), while no significant difference was observed in the protein expression of LAMA3 ($p > 0.05$) between the cells transduced with LAMA3 and LINC00628 combined and the cells that served as controls (Figure 4A).

3-(4,5-dimethyl-2-thiazolyl)-2,5-diphenyl-2-H-tetrazolium (MTT) assay was carried out to measure the proliferation of H1650 and H1299 cells. The results showed that, as compared with the cells that served as controls, LAMA3 overexpression attenuated cell proliferation ($p < 0.05$); sh-LINC00628 transfection also inhibited cell proliferation ($p < 0.05$), while cells with LINC00628 transfection displayed higher cell proliferation ($p < 0.05$). However, cell proliferation did not differ greatly between the cells that served as controls and the cells manipulated with both LAMA3 and LINC00628 combined ($p > 0.05$) (Figure 4B).

Subsequently, the scratch test was employed to measure the effects of LINC00628 on cell migration using H1650 and H1299 cell lines. The results showed that, in contrast to the cells that served as controls, the overexpression of LAMA3 inhibited the migration of H1650 and H1299 cells ($p < 0.05$), which was also significantly inhibited by LINC00628 silencing ($p < 0.05$), whereas LINC00628 overexpression significantly promoted their migration ($p < 0.05$). No significant difference was observed in the migration of H1650 cells and H1299 cells that served as controls and those transduced with both LAMA3 and LINC00628 ($p > 0.05$) (Figure 4C).

A transwell assay was used to detect the effects of LINC00628 on cell invasion using H1650 and H1299 cell lines. The results showed that LAMA3 overexpression inhibited cell invasion ($p < 0.05$), which was also significantly inhibited by sh-LINC00628 ($p < 0.05$), whereas LINC00628 overexpression promoted cell invasion ($p < 0.05$). In addition, no significant difference was observed in the cell invasion between the cells treated with LAMA3 and LINC00628 combined and the cells that served as controls ($p > 0.05$) (Figure 4D). Western blot analysis showed that, as compared with cells that served as controls, the expression of invasion-related markers (matrix metallopeptidase [MMP]2 and MMP9) as well as EMT-related protein N-cadherin and Vimentin was downregulated in cells with overexpressed LAMA3 and LINC00628 silencing and upregulated in the cells treated with LINC00628, while that of E-cadherin was elevated. However, cells transfected with overexpressed LINC00628 exhibited a contrasting trend. No significant difference was observed in the aforementioned factors in cells co-treated with LAMA3 and LINC00628 (Figure 4E).

The aforementioned results demonstrate that LINC00628 can restrain the proliferation, migration, and invasion along with EMT of lung adenocarcinoma cells by disrupting LAMA3 expression.

DNA Methylation of LAMA3 Leads to Its Low Expression in Lung Adenocarcinoma Cells

Considering methylation of a gene promoter can reduce the expression of that gene and may contribute to the development of cancer,[14–16] the methylation analysis of LAMA3 revealed the presence of a large number of CpG islands in the LAMA3 promoter (Figure 5A). Furthermore, methylation-specific PCR (MSP) was used to

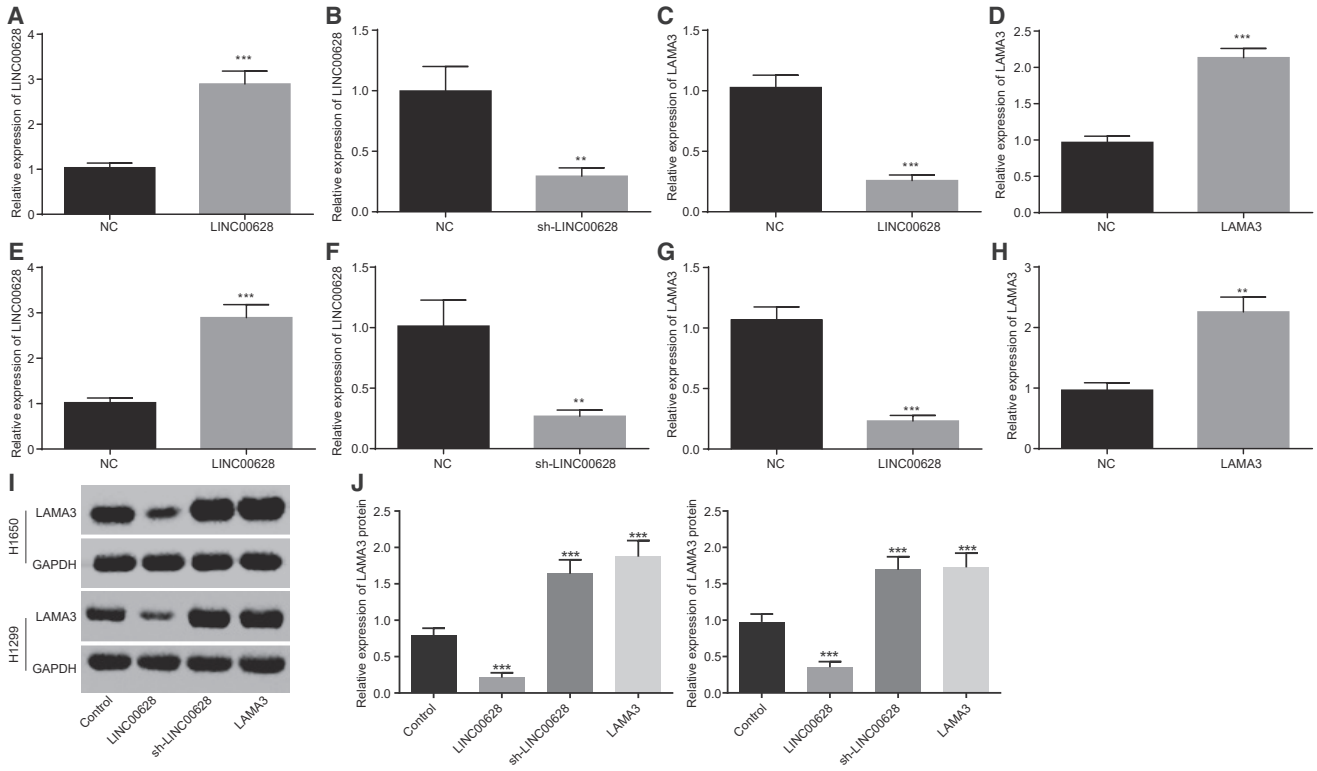

Figure 3. Overexpression of LINC00628 Inhibits LAMA3

(A) LINC00628 expression in H1650 cells transfected with overexpressed LINC00628 examined by qRT-PCR. (B) LINC00628 expression in H1650 cells transfected with silenced LINC00628 examined by qRT-PCR. (C) LAMA3 expression in H1650 cells transfected with silenced LINC00628 examined by qRT-PCR. (D) LAMA3 expression in H1650 cells transfected with overexpressed LAMA3 examined by qRT-PCR. (E) LINC00628 expression in H1299 cells transfected with overexpressed LINC00628 examined by qRT-PCR. (F) LINC00628 expression in H1299 cells transfected with silenced LINC00628 examined by qRT-PCR. (G) LINC00628 expression in H1299 cells transfected with overexpressed LAMA3 examined by qRT-PCR. (H) LAMA3 expression in H1299 cells transfected with overexpressed LAMA3 examined by qRT-PCR. (I and J) Western blot analysis of LAMA3 protein expression in H1299 cells (I) and H1650 cells (J). The statistical values were measurement data, which were expressed as mean ± SD and compared with t test; *$p < 0.05$; **$p < 0.01$; and ***$p < 0.001$ versus the cells served as NC (cells transfected with empty vector). The experiment was performed in triplicate.

study the methylation status of LAMA3 in the normal cell line BEAS-2B and the lung adenocarcinoma cell line H1650. LAMA3 exhibited a high rate of methylation in H1650 cells (Figures 5A and 5B). In order to further verify that the low expression of LAMA3 in the lung adenocarcinoma cells was due to its methylation, we added a methylation inhibitor 5-azacytidine (5-Aza) to the culture medium for lung adenocarcinoma cells and then assessed the level of methylation and LAMA3 expression in these cells using MSP and qRT-PCR. The MSP measurement showed that LAMA3 methylation was inhibited after the addition of 5-Aza (Figure 5C). Moreover, qRT-PCR and western blot analysis results verified that the expression of LAMA3 in lung adenocarcinoma cells had increased significantly after the addition of 5-Aza (Figures 5D and 5E). Moreover, MSP showed that LAMA3 in the other lung adenocarcinoma cell lines was also methylated (Figure 5F).

In summary, these results show that the methylation of LAMA3 promoter was increased in lung adenocarcinoma cell lines and resulted in its low expression in lung adenocarcinoma.

LINC00628 Recruits Methylase to Promote the DNA Methylation of LAMA3 Promoter

RNA immunoprecipitation (RIP) and chromatin immunoprecipitation (ChIP) were utilized to determine the association between LAMA3 and DNA methyltransferase (DNMT)1, DNMT3A, and DNMT3B, respectively. In order to investigate the relationship between LINC00628 and LAMA3, we used a web-based database to locate the binding site for LINC00628 in LAMA (Figure 6A). In comparison with the NC treatment, the fluorescence signal from the cells co-transfected with the wild-type LAMA3 promoter and LINC00628 was significantly decreased, while the fluorescence signal from the cells co-transfected with the mutant LAMA3 did not change significantly (Figure 6B). Because the influence of lncRNAs on the expression of their downstream target genes has been previously described as mediated by recruitment of methylated proteins, including DNMT1, DNMT3A, and DNMT3B,[17] we conducted a RIP assay to determine whether LINC00628 regulated the expression of its target genes through a similar mechanism. The results revealed that LINC00628 directly bound to DNMT1, DNMT3A, and DNMT3B in H1650 cells (Figure 6C).

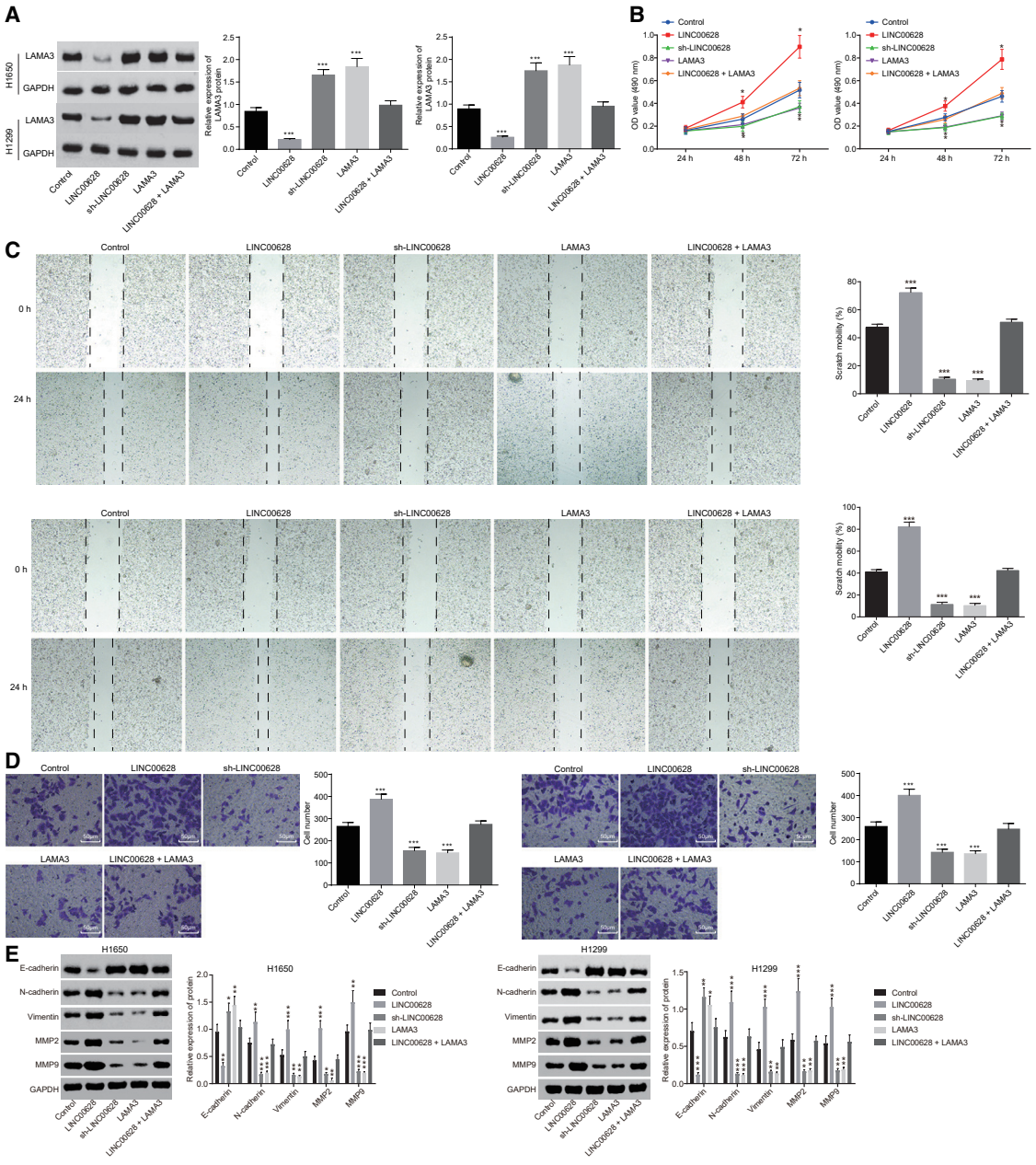

Figure 4. Reduction of LINC00628 and Overexpression of LAMA3 Suppress the Cell Proliferation, Migration, and Invasion of Lung Adenocarcinoma

(A) Western blot analysis of LAMA3 protein in H1650 cells and H1299 cells. (B) Proliferation of H1650 cells and H1299 cells, measured using MTT assay. (C) The migration of H1650 cells and H1299 cells examined by scratch assay. (D) The invasion of H1650 cells and H1299 cells detected by Transwell assay. (E) Western blot analysis of protein expression of invasion-related markers (MMP2 and MMP9) and EMT-related makers (N-cadherin, Vimentin, and E-cadherin) in H1650 cells and H1299 cells. The statistical values were measurement data, which were expressed as mean ± SD and compared with t test; *$p < 0.05$; **$p < 0.01$; and ***$p < 0.001$ versus the cells that served as controls. The experiment was performed in triplicate.

Subsequently, we detected whether LINC00628 could silence LAMA3 expression by recruiting DNMT1, DNMT3A, and DNMT3B to the promoter region of LAMA3. At first, through the application of ChIP assay, we detected the enrichment of DNMT1, DNMT3A, and DNMT3B in the LAMA3 promoter region. The results showed that the enrichment of DNMT1, DNMT3A, and DNMT3B was evidently increased in the promoter region of LAMA3 following over-expressed LINC00628 (Figure 6D). Subsequent MSP results displayed remarkably diminished methylation of LAMA3 in the H1650 cell line treated with silenced DNMT1, DNMT3A, and DNMT3B (Figure 6E).

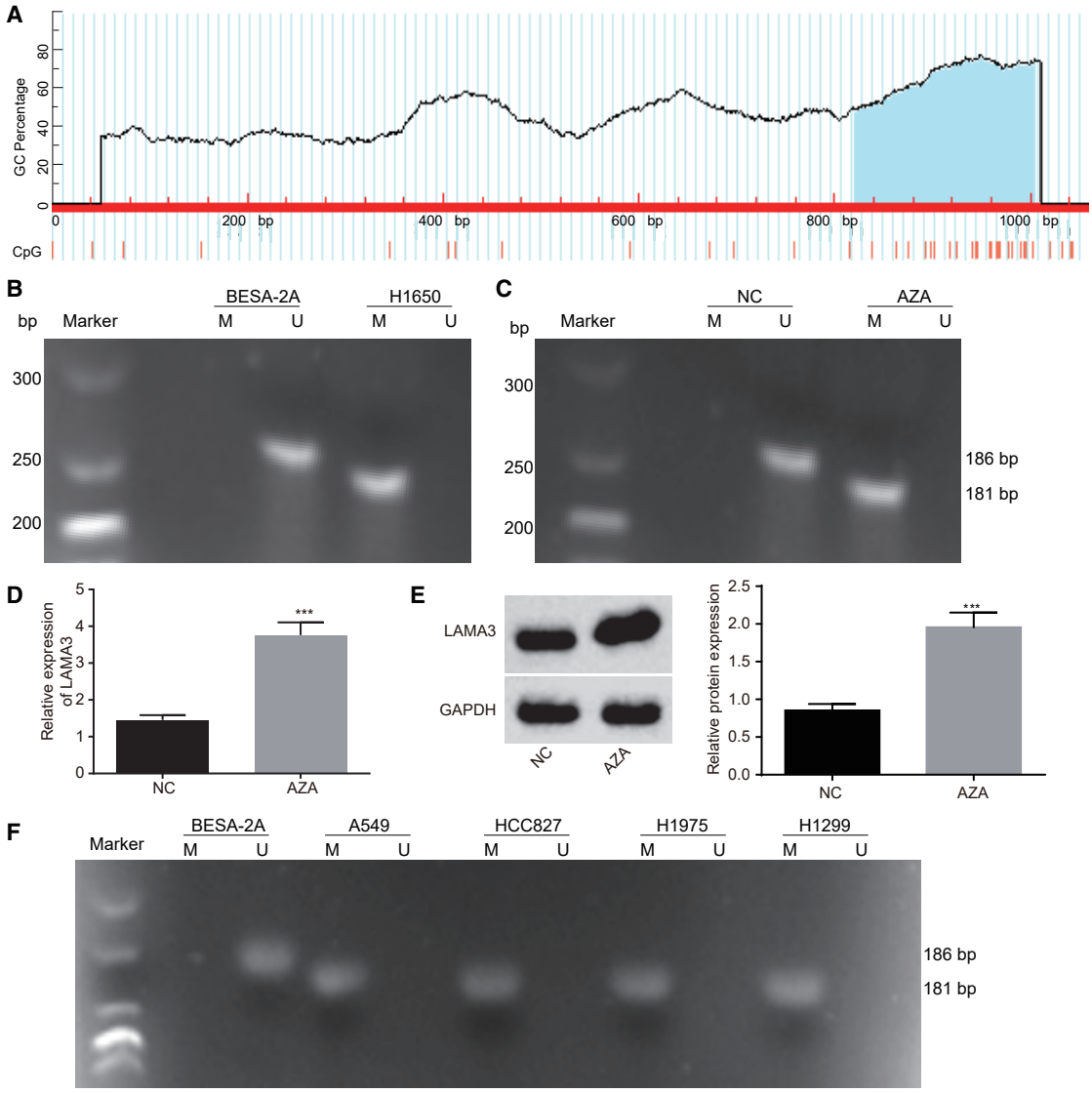

Figure 5. DNA Methylation of LAMA3 Leads to Its Low Expression in Lung Adenocarcinoma

(A) CpG islands in the LAMA3 promoter region. (B) The methylation of LAMA3 in H1650 cells examined by MSP. (C) The methylation of LAMA3 methylation in H1650 cells after 5-Aza treatment examined by MSP. (D) mRNA expression of LAMA3 in the H1650 cell line after 5-Aza treatment examined by qRT-PCR. (E) Western blot analysis of LAMA3 protein in the H1650 cell line after 5-Aza treatment. (F) Methylation of LAMA3 in BEAS-2B and other lung adenocarcinoma cell lines analyzed using MSP. The statistical values were measurement data, which were expressed as mean ± SD and compared with t test; *$p < 0.05$; **$p < 0.01$; and ***$p < 0.001$ versus BEAS-2B. The experiment was performed in triplicate.

In summary, these results show that LINC00628 could enhance the methylation of LAMA3 promoter by recruiting methylation proteins DNMT1, DNMT3A, and DNMT3B.

Inhibition of LAMA3 Promoter Methylation Inhibits Cell Proliferation, Migration, and Invasion

Western blot analysis results revealed that the protein expression of LAMA3 increased upon the addition of 5-Aza ($p < 0.05$) to H1650 and H1299 cells, and it was significantly increased in cells transfected with overexpressed LAMA3 after addition of 5-Aza ($p < 0.05$) (Figure 7A).

The results of the MTT assay indicated that the proliferation of H1650 and H1299 cells was significantly inhibited by the addition of 5-Aza ($p < 0.05$). Compared with the cells treated with overexpressed LAMA3, those treated with overexpressed LAMA3 and the addition of 5-Aza exhibited decreased cell proliferation ($p < 0.05$) (Figure 7B).

A scratch test was performed to detect the effects of LAMA3 on the migration of H1650 and H1299 cells. The results showed that cell migration was significantly inhibited by the addition of 5-Aza. In addition, cell migration was significantly inhibited

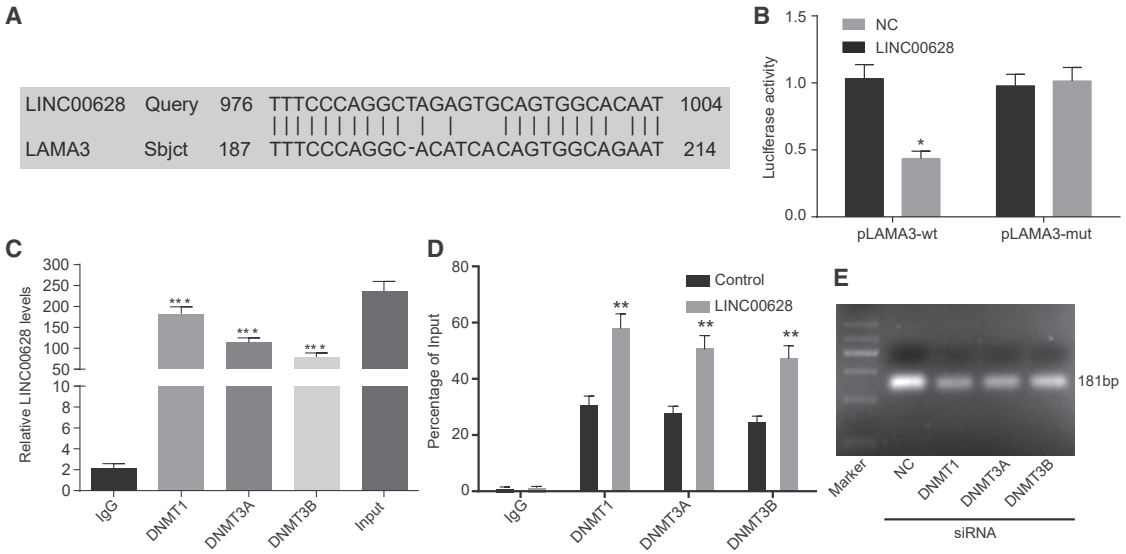

Figure 6. LINC00628 Recruits Methylase to Promote the DNA Methylation of LAMA3 Promoter

(A) Binding sites between LINC00628 and LAMA3 predicted by the bioinformatics website. (B) The binding of LINC00628 to LAMA3 promoter confirmed by dual-luciferase reporter gene assay. (C) Binding of LINC00628 to DNMT1, DNMT3A, and DNMT3B in H1650 cells detected by RIP assay. (D) Enrichment of DNMT1, DNMT3A, and DNMT3B in the promoter region of LAMA3 upon oe-LINC00628 treatment determined using ChIP assay. (E) Methylation of LAMA3 in the H1650 cell line with silenced DNMT1, DNMT3A, and DNMT3B treatment determined using MSP. The experiment was performed in triplicate. The statistical values were measurement data, which were expressed as mean ± SD and compared with t test; *$p < 0.05$; **$p < 0.01$; ***$p < 0.001$. The experiment was performed in triplicate.

by the addition of 5-Aza when LAMA3 was overexpressed (Figure 7C).

A transwell assay was performed to detect the effects of LAMA3 on the invasion of H1650 and H1299 cells. Similar to the results of the cell migration assay, the invasion of cells transfected with overexpressed LAMA3 was significantly inhibited after the addition of 5-Aza (Figure 7D). Western blot analysis demonstrated that the cells with 5-Aza treatment exhibited a decreased protein level in MMP-2, MMP-9, and E-cadherin, yet increased protein level of N-cadherin and Vimentin. The same pattern was observed in cells with LAMA3 overexpression after the addition of 5-Aza (Figure 7E).

Altogether, the above results reveal that the inhibition of LAMA3 promoter methylation could inhibit the proliferation, migration, and invasion of lung adenocarcinoma cells.

Inhibition of Methylation Enhances the Chemotherapeutic Effects of VCR on Lung Adenocarcinoma Cells

VCR is often used as a therapeutic drug in patients with lung adenocarcinoma. To further verify that the enhancement of LAMA3 methylation by LINC00628 was involved in the drug resistance of lung adenocarcinoma cells, we detected whether LINC00628 enhanced the VCR resistance of lung adenocarcinoma cells. Using an MTT assay to measure the IC_{50} of lung adenocarcinoma cells treated by both VCR and LAMA3, we found that, compared with the lung adenocarcinoma cell line H1650 transfected with empty vector, the activity of H1650 cells treated with 5-Aza and the cells treated with sh-LINC00628 was decreased, whereas the activity was increased in the cells treated with LINC00628 at the same concentration of VCR, while no significant difference was observed in the cells treated with both 5-Aza and LINC00628 (Figure 8A). Similarly, compared with the cells following empty control treatment, the IC_{50} of H1650 cells decreased significantly in response to 5-Aza treatment and sh-LINC00628 treatment but increased in response to LINC00628 treatment, while no significant difference was observed in response to the combined treatment with 5-Aza and LINC00628 (Figure 8B). A similar experiment was performed for the H1299 cells, which concluded consistent results with those of H1650 cells (Figures 8C and 8D). Altogether, these findings suggest that inhibition of methylation could strengthen the chemotherapeutic effects of VCR on lung adenocarcinoma.

Drug Resistance in Lung Adenocarcinoma Cells Is Suppressed by Reducing LINC00628 Expression

Western blot analysis results showed that, compared with cells that served as controls, the protein expression of LAMA3 in H1650 cells increased following 5-Aza treatment and sh-LINC00628 treatment but decreased following LINC00628 treatment; no significant difference was observed following the combination of 5-Aza and LINC00628 (Figure 9A).

A clonogenic assay was utilized to measure the colony formation ability of H1650 cells. The results verified that the colony formation ability of H1650 cells was obviously weakened by the addition of VCR. In comparison with cells served as controls, the colony formation ability

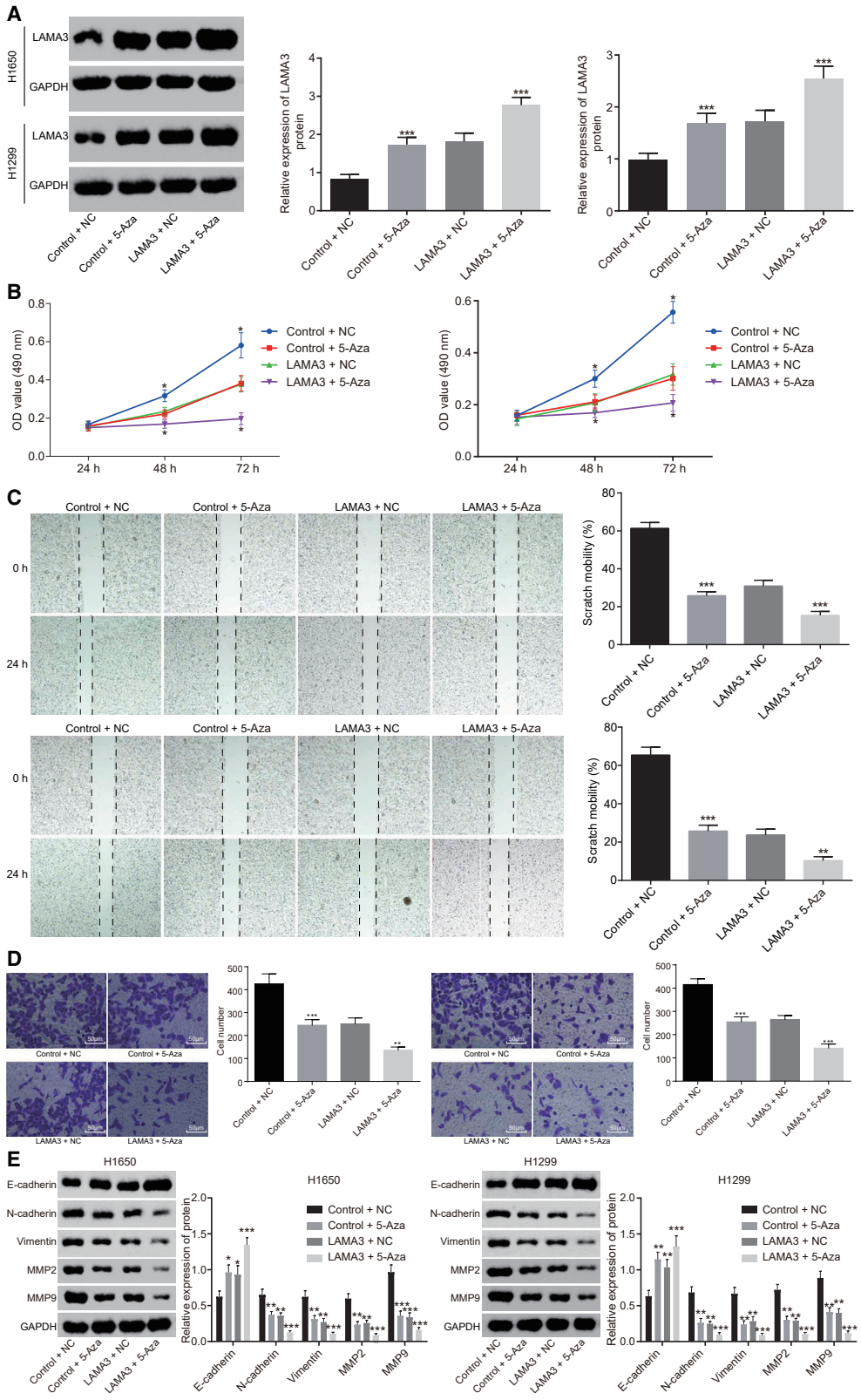

(legend on next page)

of H1650 cells in response to 5-Aza transduction and sh-LINC00628 transduction was obviously decreased, but it increased significantly in response to LINC00628 treatment, while no significant difference was observed in response to manipulation of both 5-Aza and LINC00628 (Figure 9B).

Flow cytometry was used to assess effects on the cell cycle. The results showed that the percentage of H1650 cells in the G0/G1 phase was significantly elevated after the addition of VCR, while the percentage of cells in the S and G2/M phases decreased notably. In comparison with the cells that served as controls, the percentage of cells in the G0/G1 phase was increased, but the percentage of cells in the S and G2/M phases was significantly reduced in the cells treated with 5-Aza and the cells treated with sh-LINC00628. The LINC00628 treatment led to a lower percentage of cells in the G0/G1 phase, but a greater percentage of cells in the S and G2/M phases. No significant difference was observed in the cells treated with both 5-Aza and LINC00628 (Figure 9C).

Flow cytometry was also applied to assess the effects on cell apoptosis. The results indicated that the apoptosis of H1650 cells increased obviously after the addition of VCR. In comparison with the cells that served as controls, the apoptosis of H1650 cells increased upon treatment with 5-Aza and with sh-LINC00628, but it decreased in the cells treated with LINC00628, while no significant difference was observed in the cells treated with both 5-Aza and LINC00628 (Figure 9D). Flow cytometry was also performed for the H1299 cells, and the results were consistent with those of H1650 cells (Figures 9E–9H).

Thereby, these experimental findings confirm that the reduction of LINC00628 expression could cumulatively inhibit the VCR-resistance of lung adenocarcinoma cells by suppressing LAMA3 methylation.

Inhibition of LINC00628 Suppresses Tumor Growth and Drug Resistance in Nude Mice via Reducing LAMA3 Methylation

A tumor xenograft in nude mice was used to detect the effects of LINC00628 on tumor growth. The tumor volume and malignancy of lung adenocarcinoma were detected. The results demonstrated that, after the addition of VCR, tumor growth decreased significantly ($p < 0.05$). In comparison with cells that served as controls, tumor growth decreased in response to 5-Aza treatment and sh-LINC00628 treatment, but it increased significantly in response to LINC00628 treatment ($p < 0.05$), while no significant difference was observed in response to combined treatment of 5-Aza and LINC00628 ($p > 0.05$) (Figures 10A–10C).

H&E staining was used to observe the number of tumor metastatic foci and showed that the number of foci decreased significantly after the addition of VCR ($p < 0.05$). In comparison with cells that served as controls, metastatic foci were significantly reduced in response to treatment by 5-Aza or sh-LINC00628 but increased in the response to treatment by LINC00628 ($p < 0.05$), while no significant difference was observed in response to combined 5-Aza and LINC00628 treatment ($p > 0.05$) (Figures 10D and 10E).

Western blot analysis was applied to examine the protein expression of LAMA3 in tumor tissues, and the results showed, compared with the cells that served as controls, 5-Aza treatment and sh-LINC00628 treatments increased the expression of LAMA3 in tumor tissues, while the LINC00628 treatment attenuated the expression of LAMA3 (all $p < 0.05$). No significant difference was observed in response to the treatment of combined 5-Aza and LINC00628 ($p > 0.05$) (Figures 10F and 10G).

Taken together, these results suggest that the growth and metastasis of lung adenocarcinoma cells could be inhibited by decreased LINC00628 expression, which, in turn, could result in decreased LAMA3 methylation.

DISCUSSION

Despite rapid advancements in the detection and treatment of lung cancer, it remains a major cause of cancer-related mortality worldwide, with a low overall survival rate.[18] Increasing evidence has highlighted the critical roles of lncRNAs in cancer, highlighting their potential values as therapeutic targets and biomarkers, and, at the same time, a prognostic value of DNA methylation has been demonstrated in lung adenocarcinoma.[19,20] The current study shows that the silencing of LINC00628 expression could inhibit the proliferation, invasion, migration, and drug resistance of lung adenocarcinoma cells by reducing the methylation of LAMA3 promoter.

Our results demonstrate that LINC00628 was highly expressed in lung adenocarcinoma and that its downregulation could inhibit the proliferation, invasion, and migration of lung adenocarcinoma cells. Thus we propose LINC00628 as a molecular target for impeding disease progression. Laminin-5 is often expressed in invasive lung cancer cells, and its overexpression has been established as a prognostic marker in small-sized lung adenocarcinoma, particularly in the early phase, during stage I.[21] Oncogenic roles of other lncRNAs are being discovered. The role of LINC0151 in lung adenocarcinoma is evidenced by its marked upregulation in affected tissues as compared to adjacent healthy tissues.[22] The expression of lncRNA gastric

Figure 7. Inhibition of LAMA3 Promoter Methylation Hinders the Proliferation, Migration, and Invasion of Lung Adenocarcinoma Cells

(A) The protein expression of LAMA3 in H1650 cells and H1299 cells after the addition of 5-Aza (5 μM) examined by western blot analysis. (B) Proliferation of H1650 cells and H1299 cells after the addition of 5-Aza (5 μM) detected using MTT assay. (C) Migration of H1650 cells and H1299 cells after the addition of 5-Aza (5 μM) examined by scratch assay. (D) Invasion of H1650 cells and H1299 cells after the addition of 5-Aza (5 μM) examined by Transwell assay. (E) Western blot analysis of protein expression of invasion-related markers (MMP2 and MMP9) and EMT-related makers (N-cadherin, Vimentin, and E-cadherin) in H1650 cells and H1299 cells. The experiment was performed in triplicate. The statistical values were measurement data, which were expressed as mean ± SD and compared with one-way ANOVA; *$p < 0.05$; **$p < 0.01$; and ***$p < 0.001$ compared with cells served as control and NC or the cells that served as NC treated with LAMA3.

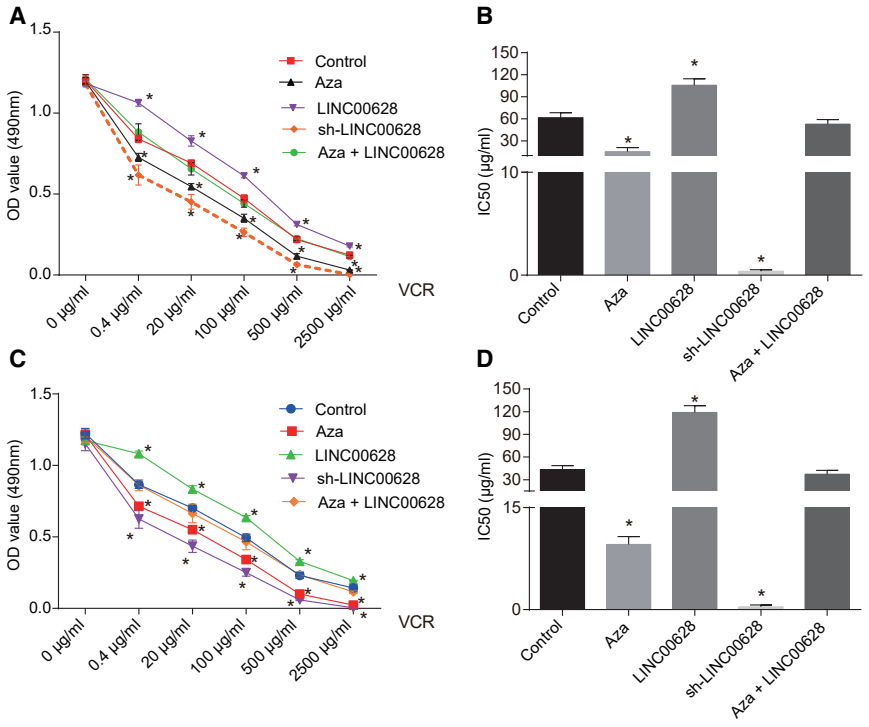

Figure 8. Inhibition of Methylation Enhances the Chemotherapeutic Effects of VCR on Lung Adenocarcinoma Cells

(A) Repression of methylation enhances VCR's effects on H1650 cells examined by MTT. The statistical values were measurement data, which were expressed as mean ± SD and compared using two-way ANOVA. The experiment was performed in triplicate. (B) LAMA3 methylation suppressed IC_{50} of VCR in H1650 cells. (C) The repression of methylation enhances VCR's effects on H1299 cells, examined by MTT. The statistical values were measurement data, which were expressed as mean ± SD and compared using two-way ANOVA. The experiment was performed in triplicate. (D) LAMA3 methylation suppressed IC_{50} of VCR in H1299 cells. The statistical values were expressed as mean ± SD and compared with one-way ANOVA; *$p < 0.05$ versus the cells that served as controls.

cancer-associated transcript 3 (GACAT3) is also significantly increased, which may play a supplementary role in stimulating the proliferation and migration of cancer cells and engender greater resistance to radiotherapy.[23]

In our study, we found that LINC00628 recruits methylase to promote LAMA3 methylation, which consequently reduces the expression of LAMA3 in lung adenocarcinoma. Others have shown that a reduction of H3K27me3 methyltransferase Ezh2 could result in the knockdown of lncRNAs in embryonic stem cells (ESCs).[24] Furthermore, lncRNAs are shown to modulate CpG DNA methylation.[25] lncRNAs, therefore, appear to play non-trivial roles in a multitude of basic biological and biochemical processes, including DNA methylation. Notably, lncRNAs and DNA methylation can conjointly lead to tumorigenesis or tumor suppression and could thus comprise a new class of cancer biomarkers.[26] Such lncRNA-mediated modulation of methylation may regulate key gene functions, as exemplified by H19 lncRNA knockdown, which activates S-adenosylho-mocysteine hydrolase (SAHH), resulting in elevated DNMT3B-mediated methylation of a lncRNA-encoding gene non-coding transcript 1 (Nctc1) within the insulin-like growth factor II gene (Igf2)-H19-Nctc1 locus.[27]

Another important finding of this study was the involvement of LAMA3 methylation in the migration and invasion of lung adenocarcinoma cells. The overexpression or demethylation of miR-1247 induced by 5-Aza treatment has been confirmed to significantly inhibit cell growth, invasion, migration, and cell cycle progression.[28] Moreover, DNA methylation markers may associate with the cell type and expression patterns of specific protein coding genes, suggesting they may possess clinical value in specific and sensitive early detection of lung cancer; however, preclinical trials are needed before translation to clinical settings.[29] Promoter hypermethylation or hypomethylation plays an important role in cancer pathogenesis by mediating gene expression.[30] It appears that DNA methylation may also comprise a molecular target for prognosis and treatment development in lung cancer.[29] Based on our results, LAMA3 methylation increases the drug resistance of lung adenocarcinoma cells. Another study has suggested that, in ovarian cancer, the methylation of the hMLH1 promoter may act as a mechanism underlying the loss of hMLH1 expression and lead to cisplatin resistance.[31] In a similar finding, cisplatin resistance in non-small cell lung cancer cells was correlated with changes in non-coding RNAs, among which AK126698 emerged as the lncRNA causing cisplatin resistance by targeting the Wnt pathway.[32] Similarly, the up-regulation of HOX antisense intergenic RNA (HOTAIR), an lncRNA directly repressed by an estrogen receptor (ER), promotes ligand-independent ER activities and contributes to tamoxifen resistance.[33] Along the same lines, lncRNA HOTAIR plays a key role in gene regulation and chromatin dynamics in a variety of cancers, while methylated forms of lncRNA MALAT1 promoter are decreased in lung cancer cells and tissues.[30]

Taken together, the present study found that the suppression of LINC00628 inhibited the proliferation, invasion, migration, and drug resistance of lung adenocarcinoma cells by reducing the methylation of LAMA3 promoter (Figure 11).

MATERIALS AND METHODS

Ethical Statement

All patients provided written informed consent prior to the study. This study was performed after approval by the Ethics Committee of the First Hospital of Qinhuangdao and was conducted in accordance with the Helsinki declaration.

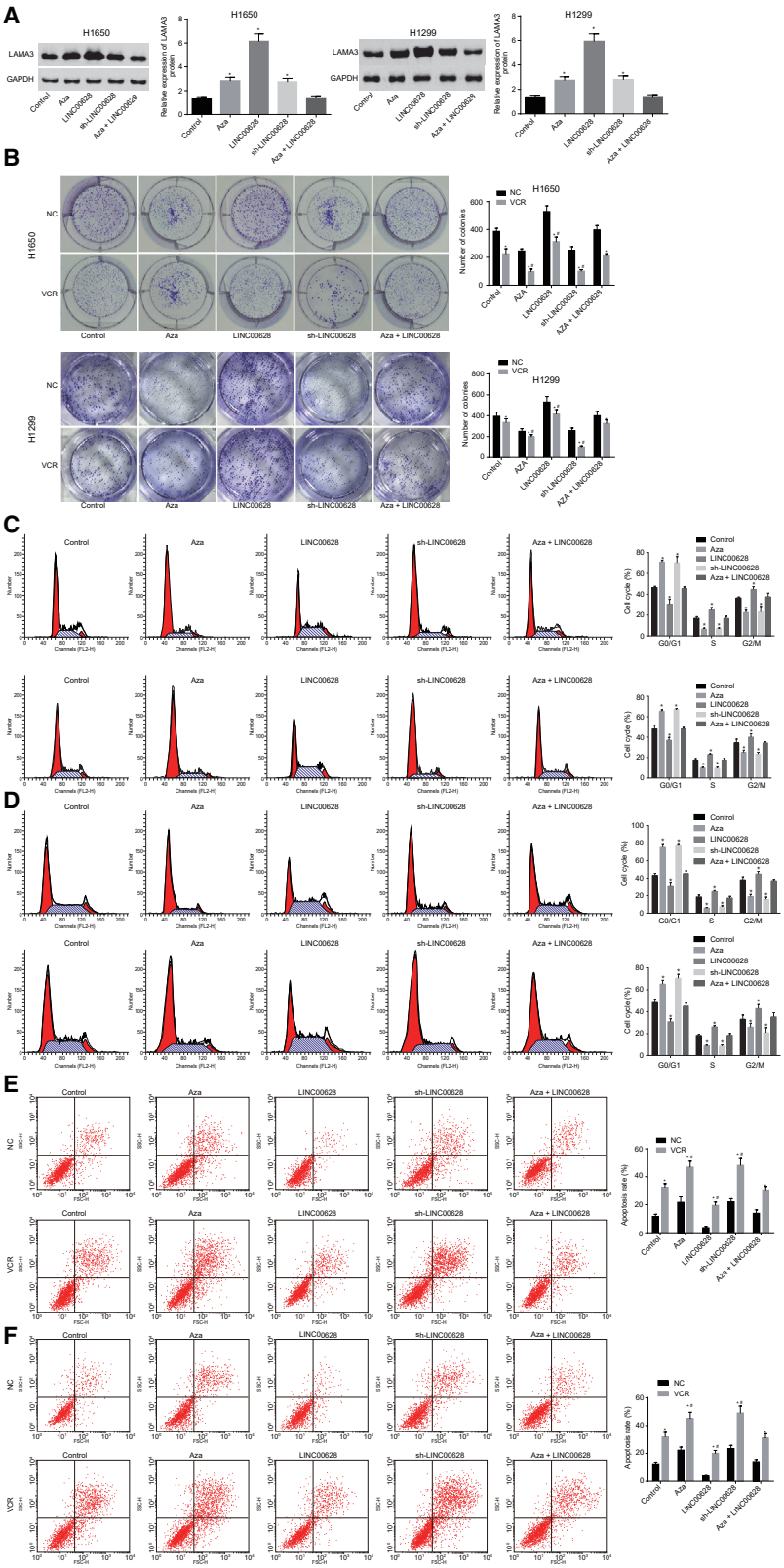

Figure 9. Downregulated LINC00628 Weakens the Resistance of Lung Adenocarcinoma Cells to VCR and Inhibits LAMA3 Methylation

(A) The protein expression of LAMA3 in H1650 cells examined by western blot analysis. (B) The colony formation ability of H1650 cells examined by clonogenic assay. (C) The cell cycle of H1650 examined by flow cytometry. (D) The apoptosis of H1650 cells examined by flow cytometry. (E) The protein expression of LAMA3 in H1299 cells examined by western blot analysis. (F) The colony formation ability of H1299 cells examined by clonogenic assay. (G) The cell cycle of H1299 examined by flow cytometry. (H) The apoptosis of H1299 cells examined by flow cytometry. The statistical values were measurement data, which were expressed as mean ± SD and compared with one-way ANOVA; *$p < 0.05$ versus the cells served as NC; $^{\#}p < 0.05$ versus the cells that served as controls. The experiment was performed in triplicate.

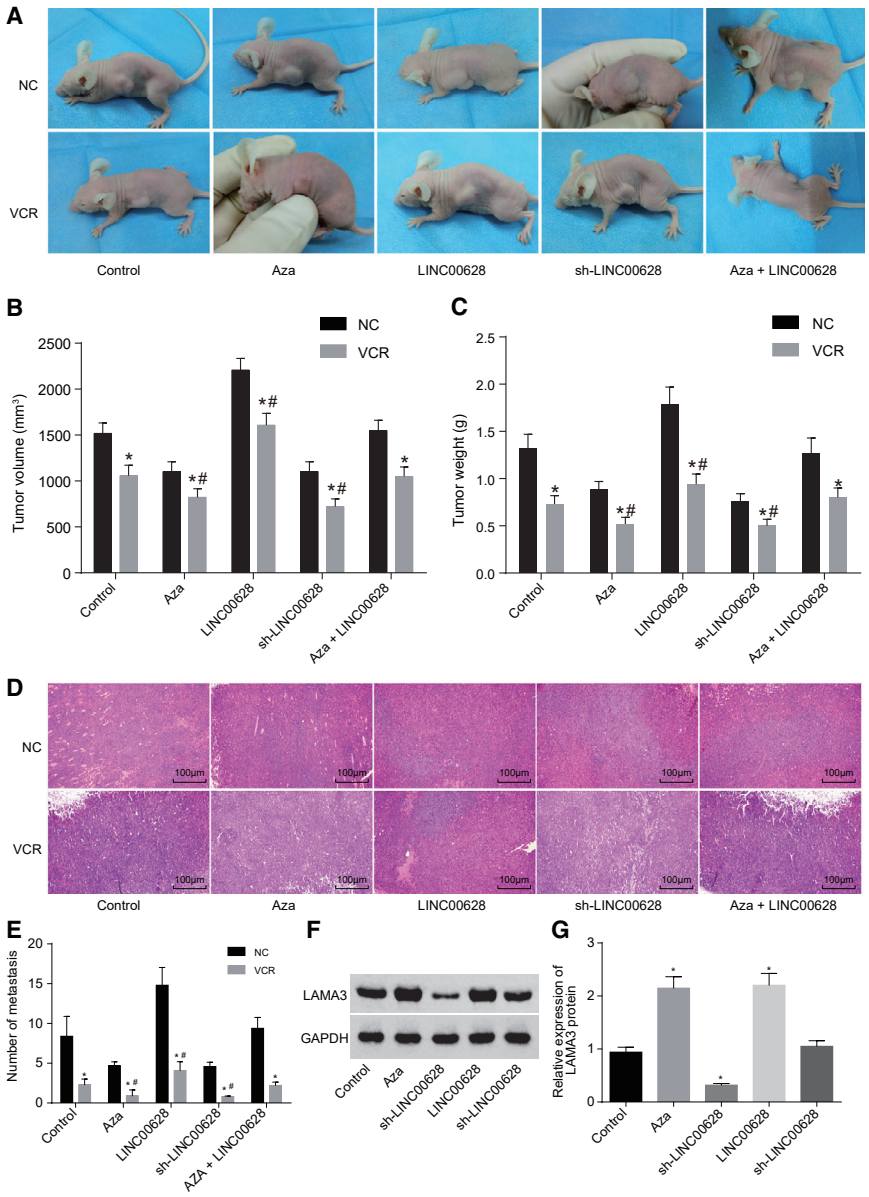

Figure 10. Decreased Expression of LINC00628 Reduces LAMA3 Methylation to Inhibit Tumor Growth and Drug Resistance in Nude Mice

(A) The transplanted tumor in nude mice. (B) The tumor volume of nude mice in each group (mm^2). (C) The tumor weight of nude mice in each group (g). (D) The metastatic tumor foci of lung adenocarcinoma cell lines examined by H&E staining. (E) The number of metastasis in each group. (F and G) Western blot analysis of LAMA3 protein expression in H1650 cells. The statistical values were measurement data, which were expressed as mean ± SD and compared with one-way ANOVA with n = 10; *p < 0.05 versus NC treatment; #p < 0.05 versus control treatment.

Study Subjects

A total of 70 patients diagnosed with lung adenocarcinoma based on pathological evidence (age: 36∼78 years), undergoing surgical resection in the First Hospital of Qinhuangdao from January 2016 to January 2017, were enrolled in this study to collect lung adenocarcinoma tissues as well as adjacent normal tissues (more than 5 cm away from the lung adenocarcinoma tissues). Prior to surgical resection, no patients were administered any adjuvant therapy. After tissue collection, the specimens were immediately frozen in liquid nitrogen and stored in a −80°C freezer until the extraction of total RNA.

Cell Culture

The human bronchial epithelial cell line BEAS-2B and human lung adenocarcinoma cell lines A549, H1650, HCC827, H1975, and H1299 were purchased from the Cell Bank of the Chinese Academy of Sciences (Shanghai, China). These cells were cultured at 37°C with 5% CO_2 in DMEM (GIBCO, Carlsbad, CA, USA) containing 10% fetal bovine serum (FBS) (GIBCO, Carlsbad, CA, USA), 100 μg/mL penicillin, and 100 μg/mL streptomycin (Invitrogen, Carlsbad, CA, USA). The cells were sub-cultured 1–2 times a week. When the cell density reached 90%, the cells were detached with 0.25% trypsin and then sub-cultured at the ratio of 1:3. The endogenous expression of LAMA3 and LINC00628 was quantified by qRT-PCR, and the two cell lines with higher expression of lncRNA LINC00628 were selected for the following experiments.

Plasmid Construction

The full-length of LINC00628 cDNA was synthesized by Realgene (Nanjing, China) and cloned into a pcDNA3.1 (+) vector (Invitrogen, Carlsbad, CA, USA). In addition, the sequence of LAMA3 was synthesized and sub-cloned into a pCDNA3.1 (+) vector (GENECHEM, Shanghai, China). Additionally, the interfering sequence of LINC00628 was synthesized and named sh-LINC00628. X-tremeGENE HP DNA transfection reagent (Roche, Basel, Switzerland) was used to transfect the plasmid vectors (pcDNA3.1-lncRNA LINC00628, and pcDNA3.1-LAMA3) into H1650 and H1299 lung adenocarcinoma cells cultured in a 6-well plate. After 48 h of transfection, the cells were collected for qRT-PCR or MTT assay.

IHC

The expression of LAMA3 in 4-μm formalin-fixed paraffin-embedded (FFPE) sections was analyzed by IHC. IHC was conducted using the staining method based on standard peroxidase. The sections were incubated at 60°C for 1 h, deparaffinized in xylene for 3 × 10 min, and hydrated in gradient ethanol (100%, 100%,

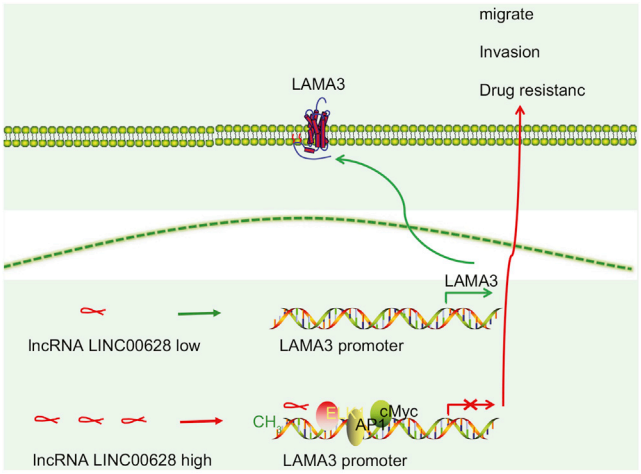

Figure 11. LINC00628 Participates in Invasion, Migration, and Drug Resistance of Lung Adenocarcinoma by Promoting Methylation of the Promoter Region of LAMA3

When LINC00628 is low expressed, the promoter of LAMA3 gene does methylate, LAMA3 expression is normal, and the function of lung gland cells is normal. In the high expression of LINC00628, LINC00628 binds to the promoter region of LAMA3 gene. Methylase is recruited to promote the methylation of LAMA3 promoter, inhibit the expression of LAMA3, and induce the migration, invasion, and chemotherapeutic resistance of lung adenocarcinoma cells.

95%, 90%, 80%, and 70%), followed by antigen retrieval by slide pretreatment in 0.01 M citrate buffer (pH = 6.0). Next, the sections were treated with 3% H_2O_2 for 10 min in order to block endogenous peroxidase. Subsequently, the sections were washed with 1 × PBS (pH = 7.4) and incubated with mouse antibody to LAMA3 (1:200, ab242197; Abcam, Cambridge, MA, USA) at 4°C overnight. Next, the sections were washed with 1 × PBS and incubated with goat anti-mouse immunoglobulin G (IgG; 1:500, ab97040; Abcam, Cambridge, MA, USA). The omission of primary antibody was taken as the NC for each sample. Finally, the immunoreactive products were visualized using 3,3-diaminobenzine. The results were evaluated using System Microscope IX71 (Olympus America, Center Valley, PA, USA).[34]

Protein Extraction and Western Blot Analysis

After homogenization, total cellular protein was extracted from the lung adenocarcinoma and the adjacent normal tissues using protein kits (Pierce Biotechnology, Rockford, IL, USA). The total protein concentration in the tissue homogenate was measured using the bicinchoninic acid protein assay kit (Shenergy Biocolor, Shanghai, China). A total of 50 μg protein from the samples was then separated using 10%–15% sodium dodecyl sulfate polyacrylamide gel electrophoresis and transferred onto the polyvinylidene difluoride membranes (Roche Diagnostics, Indianapolis, IN, USA). The membranes were incubated with 5% skimmed milk in PBS for 2 h and then incubated with mouse antibodies to LAMA3, MMP2, MMP9, E-cadherin, and Vimentin at 4°C overnight. On the following day, the membranes were washed with PBS and incubated with goat anti-mouse horseradish peroxidase-conjugated IgG (1:1,000). The immunoreactive products were visualized using enhanced chemiluminescence detection kits (Pierce Biotechnology, Rockford, IL, USA) and quantified by grayscale analysis.[35]

Cell Treatments

All plasmids were constructed by the Shanghai Biotechnology Company (Shanghai, China). A day before transfection, H1650 and H1299 cells were seeded into a 6-well plate. Upon 50% cell confluence, the cells were transfected using Lipofectamine 2000 (11668-019, Invitrogen, NY, USA) in accordance with the operational instructions provided by the manufacturer. In brief, the plasmids (100 pmol at a final concentration of 50 nM in each well) were diluted in 250 μL serum-free medium Opti-MEM (51985042, GIBCO, Gaitherburg, MD, USA). Simultaneously, 5 μL Lipofectamine 2000 was diluted in fresh 250 μL serum-free medium Opti-MEM and incubated at room temperature for 5 min. Next, the two solutions were mixed and incubated at room temperature for 20 min. Next, the cells were cultured with the mixed solutions at 37°C with 5% CO_2 for 6–8 h, and the transfection medium was replaced with a complete medium. The cells were finally harvested 24–48 h post transfection and used for subsequent experiments.

To study the effect of 5-Aza (Sigma-Aldrich, St. Louis, MO, USA), H1650 and H1299 cells were treated with 10 μM 5-Aza for 72 h prior to subsequent experiments. In order to determine the sensitivity of H1650 and H1299 cells to VCR, the cells were treated by VCR 24 h prior to the experiments.

FISH Assay

Sub-cell localization of LINC00628 was detected using a FISH Kit (Roche, Basel, Switzerland). In brief, transfected H1650 cells were washed twice with pre-cooled PBS and fixed in 4% paraformaldehyde. Subsequently, digoxin-labeled LINC00628 probes (Sigma-Aldrich, St. Louis, MO, USA) were added into the cell culture medium for hybridization. The cell nuclei were then stained with DAPI for 10 min at room temperature (Sigma, St. Louis, MO, USA). Subsequently, the cells were washed twice with pre-cooled PBS before being photographed under a laser confocal microscope (FV1000, Olympus, Tokyo, Japan). The experiment was performed in triplicate.

Dual-Luciferase Reporter Gene Assay

The National Center for Biotechnology Information (NCBI) database (https://www.ncbi.nlm.nih.gov/gene) was used to determine the sequence of the LAMA3 promoter and the full-length sequence of LINC00628 gene. The LAMA3 promoter, pLAMA3, was then cloned into a psiCheck2 plasmid downstream of the luciferase reporter gene. Next, the empty vector and LINC00628 were each transfected into H1650 cells. Luciferase activity was measured using a luciferase assay kit (Promega, Madison, WI, USA), and the effect was expressed as relative fluorescent enzyme activity with the target sequence. After 48 h of incubation, the cells were lysed in 1 × passive lysate, and the luciferase activity of transfected cells was measured using a

Table 2. Sequences of Primers

Primer	Sequence
lncRNA LINC00628	Forward: 5′-ACTCCGCCTGGATGGGAATA-3′
	Reverse: 5′-TGGCAGTCTCCCCAAGTAGA-3′
LAMA3-M	Forward: 5′-GCCCAAGCCTCCTGATTTCT-3′
	Reverse: 5′-CAATGCAGCCCTTGTAGGGA-3′
LAMA3-U	Forward: 5′-TTGTGGGATGCCTGAGGAAC-3′
	Reverse: 5′-CATCAAAGCTGATGTGCCCG-3′
GAPDH	Forward: 5′-TCGACAGTCAGCCGCATCTTCTTT-3′
	Reverse: 5′-ACCAAATCCGTTGACTCCGACCTT-3′

GAPDH, glyceraldehyde-3-phosphate dehydrogenase; LAMA3, LAMA3, laminin subunit alpha 3; M, methylated; U, unmethylated; lncRNA, long non-coding RNA

dual-luciferase reporter gene assay system (Promega, Madison, WI, USA), in which both the firefly luciferase activity of the target gene and the Renilla luciferase activity of the internal control were measured. The experiment was performed in triplicate.

RIP

RIP analysis was performed using a protein immune-precipitation kit (Millipore, Billerica, MA, USA) according to the manufacturer's instructions. H1650 cells were lysed in the RIP lysis buffer. Next, the cells were centrifuged at 20,000 × *g* at 4°C for 10 min to collect the supernatant. Subsequently, the cells were incubated overnight at 4°C with anti-IgG (1:300, ab109489; Abcam, Cambridge, UK), DNMT1 antibody (1:100, ab13537; Abcam, Cambridge, UK), DNMT3A antibody (1:100, ab2850; Abcam, Cambridge, UK), and DNMT3B antibody (1:100, ab2851; Abcam, Cambridge, UK). Proteins and RNA complexes were precipitated using Pierce protein A/G Magnetic Beads (88803, Thermo Fisher Scientific, Waltham, MA, USA). The protein samples were detached with protease K to extract the RNA for subsequent qRT-PCR.

ChIP Assay

According to the manufacturer's instructions, a ChIP assay was conducted using an EZ-Magna Chip A Kit (Millipore, Boston, MA, USA). Subsequently, 1×10^7 H1650 cells were cross-linked with 1% formaldehyde for 10 min at room temperature. In the next step, 200–1,000 bp DNA fragments were obtained through ultrasonic treatment over ice. The cells were centrifuged at 12,000 × *g* for 10 min to collect the supernatant. After that, the cells were incubated with anti-IgG (1:300, ab109489; Abcam, Cambridge, UK), anti-DNMT1 antibody (1:100, ab2850; Abcam, Cambridge, UK), anti-DNMT3B antibody (1:100, ab2851, Abcam, Cambridge, UK), and anti-H3K27me3 antibody (1:100, Abcam, Cambridge, UK) at 4°C overnight. The complexes of proteins and DNA were precipitated using Pierce protein A/G Magnetic Beads (88803, Thermo Fisher Scientific, Waltham, MA, USA). After de-crosslinking at 65°C overnight, DNA was extracted using phenol chloroform, purified, and collected for qRT-PCR. The primer sequences used were as follows: forward 5′-AAGATCCCAGGCTCCCGTT-3′ and reverse 5′-GCCG CTCCCCTTGCTCCAC-3′.

Methylation Analysis

The DNA in the cells was extracted using a DNeasy blood and tissue kit or a QIAamp DNA FFPE kit (QIAGEN, Hilden, Germany) according to the manufacturer's instructions. An EZ DNA Methylation-Gold Kit (Zymo Research, Irvine, CA, USA) was then used to convert and purify 500 ng DNA extracted from the cells. The EpiTect PCR Control DNA set (QIAGEN, Valencia, CA, USA) was used to regulate methylation and unmethylation. Subsequently, DNA was treated with hydrosulfite. All unmethylated cytosine was transformed into uracil. Dimethylated cytosine was subjected to MSP. The PCR primers are shown in Table 2. Here, LAMA3-M refers to the primers designed for methylated DNA, and LAMA3-U refers to primers designed for unmethylated DNA. ExTaq polymerase was premixed with a PCR Kit (Takara, Bio), and 25 μL mixture was used for PCR amplification, according to the manufacturer's instructions. The reaction conditions were as follows: 95°C, 10 min; 94°C, 30 s; 60°C, 30 s; 72°C 60 s (30 cycles), and then extension at 72°C for 10 min. Additionally, the PCR products were resolved through 3% agarose gel electrophoresis in conjunction with ethidium bromide. If fragments were obtained through amplification after the hydrosulfite-treated DNA was methylated, it indicated that DNA in the gene was methylated; otherwise, the DNA was considered unmethylated.

Scratch Test

H1650 and H1299 cells were seeded into a 6-well plate at a density of 2×10^5 cells/well and cultured for 24 h. A sterile 200 μL pipette tip was then used to generate a straight scratch on the cell layer in each well. The cells were then incubated in fresh medium (containing 2% serum) at 37°C, 5% CO_2, and saturated humidity for 48 h. Subsequently, the wound area that remained unpopulated by migrating cells after 48 h of wound creation was measured using ImageJ software. Each experiment was performed in triplicate.

Transwell Assay

H1650 and H1299 cell suspensions (200 μL, 2×10^5 cells/mL) were added into the apical chamber of a 24-well Transwell plate containing an 8-μm polycarbonate filter membrane (Costar, Corning, NY, USA) in each well. The cells served as controls comprised of cells treated with DMEM (containing 10% FBS). In the experimental group, 500 μL DMEM containing recombinant human LAMA3 (200 ng/mL) was introduced into the basolateral chamber. Subsequently, the cells were incubated for 24 h at 37°C with 5% CO_2 in a humidified environment. Each group had 3 duplicate wells. After incubation, the medium was removed from the apical chamber and the cells in each group were scraped with cotton swabs. Subsequently, the cells were transferred onto the surface of a membrane, fixed with 4% paraformaldehyde for 20 min, and then stained with 0.1% crystal violet for 5 min. Finally, 5 visual fields were randomly selected from each well, and the number of invasive cells was counted with 200× magnification under a microscope. Each experiment was performed in triplicate.

MTT Assay

H1650 and H1299 cells were seeded in a 96-well plate at a density of 1×10^4 cells/well and incubated in a 5% CO_2 incubator at 37°C

overnight. Next, the cells were incubated for 24 h in a medium containing 10% FBS and 0, 4, 20, 100, 500, and 2500 μg/mL VCR (KeyGEN Biotech, Nanjing, China). Simultaneously, the IC_{50} of VCR was determined. Subsequently, 10 μL MTT (0.5 mg/mL) was added to each well for 4-h incubation, and the supernatant was then removed, followed by the addition of 200 μL DMSO to terminate the reaction. The cells were then incubated for another 15 min at 37°C, and the optical density (OD) value of each well was detected at a wavelength of 490 nm using a Bio-Rad platereader (Hercules, CA, USA). Each experiment was conducted in triplicate.

Clonogenic Assay

H1650 and H1299 cells were seeded in a 24-well plate (200 cells/well) and cultured for 12 h before treatment with 30 μg/mL VCR. Following that, the cells were incubated at 37°C with 5% CO_2 for 15 days, and the medium was changed every 2 days. After 2 washes with PBS, the cells were fixed for 15 min in 75% methanol and then treated with 1% methyl chloride onium aniline. Finally, an inverted microscope was used to count the number of visible colonies. The relative ability of colony formation = (the average number of experimental clones/the average number of clones) × 100%.

Flow Cytometry

H1650 and H1299 cells were cultured in a 6-well plate for 24 h and transfected for 48 h. Subsequently, the cells were incubated with 30 μg/mL VCR at 37°C with 5% CO_2 for 24 h. After washing with PBS, the cells were collected and fixed in 70% ethanol at 4°C overnight. In the next step, the cells were washed with PBS and suspended in AnnexinV-fluoresceine isothiocyanate (FITC) (BD Company, USA) and incubated at room temperature in conditions devoid of light. After 15 min of incubation devoid of light at room temperature, the cells were immediately analyzed by flow cytometry (Beckman Coulter, USA).

RNA Extraction and Quantification

TRIzol reagent (Invitrogen, Carlsbad, CA, USA) was used to separate the total RNA from the samples, following manufacturer's instructions. Next, a reverse transcription kit (Takara, Dalian, China) was used to reverse transcribe the isolated RNA into cDNA. qRT-PCR was performed using an ABI 7500 device (Applied Biosystems, Foster City, CA, USA). The PCR reaction conditions were as follows: 2 min at 50°C, 10 min at 95°C, 15 s at 95°C, and 30 s at 60°C. qRT-PCR was standardized based on the expression of glyceraldehyde 3-phosphate dehydrogenase (GAPDH). The PCR primers are shown in Table 2. The $2^{-\Delta\Delta Ct}$ method was used to calculate the relative expressions of the target genes. All qRT-PCR reactions were conducted in triplicates.

Tumorigenicity Assay in Nude Mice

A total of 50 4-week-old mice (18–25 g, BALB/c) were purchased from Chinese PLA General Hospital Laboratory Animal and used in this study. The mice were kept in a controlled environment with a set temperature of 23 ± 2°C, set humidity of 60 ± 5%, and an alternative cycle of 12 h day and light period with free access to sterilized food and water. Next, H1650 cells in the logarithmic growth phase in each group were collected, and a 5×10^7 cells/mL cell suspension was made. Then 0.2 mL of each suspension was injected subcutaneously into a BALB/c mouse using a 1 mL syringe. In the fourth week after injection, the maximum diameter (L) and minimum diameter (W) of the tumor in each mouse were measured using a Vernier caliper in order to calculate the tumor volume using the formula: $V = W^2 \times L \times 0.52$. Thirty days after tumor inoculation, the nude mice were sacrificed, and the tumors were isolated and weighed on a small scale. In order to observe the metastasis of lung adenocarcinoma cells, H&E staining was used to examine cellular morphology and record the number of metastatic tumor foci on the lung surface under a microscope.

Statistical Analysis

All statistical analyses were conducted using the SPSS 18 software (IBM, Armonk, NY, USA). Descriptive data were expressed as mean ± SD. The data were analyzed using t test, one-way ANOVA, and chi-square test. A p value of < 0.05 was considered statistically significant.

AUTHOR CONTRIBUTIONS

S.-F.X., Y.Z., and L.Z. designed the study. P.W. and L.-M.G. collated the data and designed and developed the database. X.-B.Y., S.-S.S., and L.Z. carried out data analyses and produced the initial draft of the manuscript. C.-M.N., T.W., and Q.T. contributed to drafting the manuscript. All authors read and approved the final submitted manuscript.

CONFLICTS OF INTEREST

The authors declare no competing interests.

ACKNOWLEDGMENTS

This study was supported by the Key Medical Science Research Plan of the Health Department of Hebei Province (No. 20130289). We acknowledge and appreciate our colleagues for their valuable efforts and comments on this paper.

REFERENCES

1. Imielinski, M., Berger, A.H., Hammerman, P.S., Hernandez, B., Pugh, T.J., Hodis, E., Cho, J., Suh, J., Capelletti, M., Sivachenko, A., et al. (2012). Mapping the hallmarks of lung adenocarcinoma with massively parallel sequencing. Cell *150*, 1107–1120.

2. Wilkerson, M.D., Yin, X., Walter, V., Zhao, N., Cabanski, C.R., Hayward, M.C., Miller, C.R., Socinski, M.A., Parsons, A.M., Thorne, L.B., et al. (2012). Differential pathogenesis of lung adenocarcinoma subtypes involving sequence mutations, copy number, chromosomal instability, and methylation. PLoS ONE *7*, e36530.

3. Cancer Genome Atlas Research Network (2014). Comprehensive molecular profiling of lung adenocarcinoma. Nature *511*, 543–550.

4. Ding, L., Getz, G., Wheeler, D.A., Mardis, E.R., McLellan, M.D., Cibulskis, K., Sougnez, C., Greulich, H., Muzny, D.M., Morgan, M.B., et al. (2008). Somatic mutations affect key pathways in lung adenocarcinoma. Nature *455*, 1069–1075.

5. Zhao, J., Sun, Y., Huang, Y., Song, F., Huang, Z., Bao, Y., Zuo, J., Saffen, D., Shao, Z., Liu, W., and Wang, Y. (2017). Functional analysis reveals that RBM10 mutations contribute to lung adenocarcinoma pathogenesis by deregulating splicing. Sci. Rep. *7*, 40488.

6. Wu, Y., Liu, H., Shi, X., Yao, Y., Yang, W., and Song, Y. (2015). The long non-coding RNA HNF1A-AS1 regulates proliferation and metastasis in lung adenocarcinoma. Oncotarget *6*, 9160–9172.

7. Gutschner, T., Hämmerle, M., Eissmann, M., Hsu, J., Kim, Y., Hung, G., Revenko, A., Arun, G., Stentrup, M., Gross, M., and et al. (2013). The noncoding RNA MALAT1 is a critical regulator of the metastasis phenotype of lung cancer cells. Cancer Res. *73*, 1180–1189.

8. Shen, Y., Wang, Z., Loo, L.W., Ni, Y., Jia, W., Fei, P., Risch, H.A., Katsaros, D., and Yu, H. (2015). LINC00472 expression is regulated by promoter methylation and associated with disease-free survival in patients with grade 2 breast cancer. Breast Cancer Res. Treat. *154*, 473–482.

9. Yang, B., Yang, Z.G., Gao, B., Shao, G.G., and Li, G.H. (2015). 5-Aza-CdR can reverse gefitinib resistance caused by DAPK gene promoter methylation in lung adenocarcinoma cells. Int. J. Clin. Exp. Pathol. *8*, 12961–12966.

10. Virolle, T., Coraux, C., Ferrigno, O., Cailleteau, L., Ortonne, J.P., Pognonec, P., and Aberdam, D. (2002). Binding of USF to a non-canonical E-box following stress results in a cell-specific derepression of the lama3 gene. Nucleic Acids Res. *30*, 1789–1798.

11. Moller-Levet, C.S., Betts, G.N., Harris, A.L., Homer, J.J., West, C.M., and Miller, C.J. (2009). Exon array analysis of head and neck cancers identifies a hypoxia related splice variant of LAMA3 associated with a poor prognosis. PLoS Comput. Biol. *5*, e1000571.

12. Abrass, C.K., Berfield, A.K., Ryan, M.C., Carter, W.G., and Hansen, K.M. (2006). Abnormal development of glomerular endothelial and mesangial cells in mice with targeted disruption of the lama3 gene. Kidney Int. *70*, 1062–1071.

13. Zhou, C., Zhu, Y., Lu, B., Zhao, W., and Zhao, X. (2018). Survivin expression modulates the sensitivity of A549 lung cancer cells resistance to vincristine. Oncol. Lett. *16*, 5466–5472.

14. Wang, D., Li, C., and Zhang, X. (2014). The promoter methylation status and mRNA expression levels of CTCF and SIRT6 in sporadic breast cancer. DNA Cell Biol. *33*, 581–590.

15. Gao, L., Qi, X., Hu, K., Zhu, R., Xu, W., Sun, S., Zhang, L., Yang, X., Hua, B., and Liu, G. (2016). Estrogen receptor β promoter methylation: a potential indicator of malignant changes in breast cancer. Arch. Med. Sci. *12*, 129–136.

16. Shao, L., Chen, Z., Peng, D., Soutto, M., Zhu, S., Bates, A., Zhang, S., and El-Rifai, W. (2018). Methylation of the HOXA10 Promoter Directs miR-196b-5p-Dependent Cell Proliferation and Invasion of Gastric Cancer Cells. Mol. Cancer Res. *16*, 696–706.

17. Vispé, S., Deroide, A., Davoine, E., Desjobert, C., Lestienne, F., Fournier, L., Novosad, N., Bréand, S., Besse, J., Busato, F., et al. (2015). Consequences of combining siRNA-mediated DNA methyltransferase 1 depletion with 5-aza-2′-deoxycytidine in human leukemic KG1 cells. Oncotarget *6*, 15265–15282.

18. Mino-Kenudson, M., Chirieac, L.R., Law, K., Hornick, J.L., Lindeman, N., Mark, E.J., Cohen, D.W., Johnson, B.E., Jänne, P.A., Iafrate, A.J., and Rodig, S.J. (2010). A novel, highly sensitive antibody allows for the routine detection of ALK-rearranged lung adenocarcinomas by standard immunohistochemistry. Clin. Cancer Res. *16*, 1561–1571.

19. Qiu, M., Feng, D., Zhang, H., Xia, W., Xu, Y., Wang, J., Dong, G., Zhang, Y., Yin, R., and Xu, L. (2016). Comprehensive analysis of lncRNA expression profiles and identification of functional lncRNAs in lung adenocarcinoma. Oncotarget *7*, 16012–16022.

20. Xia, W., Chen, Q., Wang, J., Mao, Q., Dong, G., Shi, R., Zheng, Y., Xu, L., and Jiang, F. (2015). DNA methylation mediated silencing of microRNA-145 is a potential prognostic marker in patients with lung adenocarcinoma. Sci. Rep. *5*, 16901.

21. Moriya, Y., Niki, T., Yamada, T., Matsuno, Y., Kondo, H., and Hirohashi, S. (2001). Increased expression of laminin-5 and its prognostic significance in lung adenocarcinomas of small size. An immunohistochemical analysis of 102 cases. Cancer *91*, 1129–1141.

22. Chen, J., Zhang, F., Wang, J., Hu, L., Chen, J., Xu, G., and Wang, Y. (2017). LncRNA LINC01512 Promotes the Progression and Enhances Oncogenic Ability of Lung Adenocarcinoma. J. Cell. Biochem. *118*, 3102–3110.

23. Yang, X., Zhang, W., Cheng, S.Q., and Yang, R.L. (2018). High expression of lncRNA GACAT3 inhibits invasion and metastasis of non-small cell lung cancer to enhance the effect of radiotherapy. Eur. Rev. Med. Pharmacol. Sci. *22*, 1315–1322.

24. Wu, S.C., Kallin, E.M., and Zhang, Y. (2010). Role of H3K27 methylation in the regulation of lncRNA expression. Cell Res. *20*, 1109–1116.

25. Berghoff, E.G., Clark, M.F., Chen, S., Cajigas, I., Leib, D.E., and Kohtz, J.D. (2013). Evf2 (Dlx6as) lncRNA regulates ultraconserved enhancer methylation and the differential transcriptional control of adjacent genes. Development *140*, 4407–4416.

26. Du, Z., Fei, T., Verhaak, R.G., Su, Z., Zhang, Y., Brown, M., Chen, Y., and Liu, X.S. (2013). Integrative genomic analyses reveal clinically relevant long noncoding RNAs in human cancer. Nat. Struct. Mol. Biol. *20*, 908–913.

27. Zhou, J., Yang, L., Zhong, T., Mueller, M., Men, Y., Zhang, N., Xie, J., Giang, K., Chung, H., Sun, X., et al. (2015). H19 lncRNA alters DNA methylation genome wide by regulating S-adenosylhomocysteine hydrolase. Nat. Commun. *6*, 10221.

28. Zhang, J., Fu, J., Pan, Y., Zhang, X., and Shen, L. (2016). Silencing of miR-1247 by DNA methylation promoted non-small-cell lung cancer cell invasion and migration by effects of STMN1. OncoTargets Ther. *9*, 7297–7307.

29. Lu, F., and Zhang, H.T. (2011). DNA methylation and nonsmall cell lung cancer. Anat. Rec. (Hoboken) *294*, 1787–1795.

30. Guo, F., Guo, L., Li, Y., Zhou, Q., and Li, Z. (2015). MALAT1 is an oncogenic long non-coding RNA associated with tumor invasion in non-small cell lung cancer regulated by DNA methylation. Int. J. Clin. Exp. Pathol. *8*, 15903–15910.

31. Strathdee, G., MacKean, M.J., Illand, M., and Brown, R. (1999). A role for methylation of the hMLH1 promoter in loss of hMLH1 expression and drug resistance in ovarian cancer. Oncogene *18*, 2335–2341.

32. Yang, Y., Li, H., Hou, S., Hu, B., Liu, J., and Wang, J. (2013). The noncoding RNA expression profile and the effect of lncRNA AK126698 on cisplatin resistance in non-small-cell lung cancer cell. PLoS ONE *8*, e65309.

33. Xue, X., Yang, Y.A., Zhang, A., Fong, K.W., Kim, J., Song, B., Li, S., Zhao, J.C., and Yu, J. (2016). LncRNA HOTAIR enhances ER signaling and confers tamoxifen resistance in breast cancer. Oncogene *35*, 2746–2755.

34. Qin, H., Zhou, J., Zhou, P., Xu, J., Tang, Z., Ma, H., and Guo, F. (2016). Prognostic significance of RelB overexpression in non-small cell lung cancer patients. Thorac. Cancer *7*, 415–421.

35. Ni, R.S., Shen, X., Qian, X., Yu, C., Wu, H., and Gao, X. (2012). Detection of differentially expressed genes and association with clinicopathological features in laryngeal squamous cell carcinoma. Oncol. Lett. *4*, 1354–1360.